IEEE Access
Multidisciplinary ⋮ Rapid Review ⋮ Open Access Journal

Received April 7, 2022, accepted April 21, 2022, date of publication April 29, 2022, date of current version May 9, 2022.

Digital Object Identifier 10.1109/ACCESS.2022.3171323

A Novel Model of Partial Discharge Initiation in Cable Insulation

GEN LI[1], JIE CHEN[2], HONGZE LI[3], LIBIN HU[2], WENJUN ZHOU[1], (Senior Member, IEEE), AND CHENGKE ZHOU[1,4]

[1]School of Electrical Engineering and Automation, Wuhan University, Wuhan 430072, China
[2]Electric Power Research Institute, State Grid Jiangsu Electric Power Company, Nanjing 211103, China
[3]State Grid Jiangsu Electric Power Company, Nanjing 211103, China
[4]School of Computing, Engineering and Built Environment, Glasgow Caledonian University, Glasgow G4 0BA, U.K.

Corresponding author: Chengke Zhou (c.zhou@gcu.ac.uk)

This work was supported in part by the State Grid under Project 5700-202118195A-0-0-00.

ABSTRACT Urban power transmission and distribution rely on safe operation of vast network of power cables. Majority cable insulation defects can result in partial discharge (PD), which is therefore a degradation mechanism as well as a good indicator of cable insulation condition. Previously published PD models, however, failed to help quantitatively evaluate the insulation condition, or they fail to help differentiate those in between the conditions which are safe to operate from those which may need urgent testing or inspection. PD mechanisms in power cables are reviewed first in this paper. Then a novel model which is based on F distribution is proposed aiming to classify the PD activities which may be associated with different level of degradation. This is based on previous reports that PD activities manifests differently when the levels of degradation of the defect site(s) progress. After that, the features and effects of the model are presented with a case study, and the model is verified by analyzing the waveform similarities. Finally, the nature of the model is compared with the abc-model and the dipole model, demonstrating that proposed model can uniquely recognize the three stages of PD defect development.

INDEX TERMS Cable insulation, condition monitoring, partial discharges, abc-model, dipole model.

I. INTRODUCTION

Electric power transmission and distribution rely on vast networks of high voltage (HV) and medium voltage (MV) cables for power delivery [1]. Power cables are subject to electrical, thermal, mechanical, and environmental stresses, which result in insulation degradation or defects constantly when in service. In condition monitoring, partial discharge (PD) measurement has been used extensively to assess the condition of insulating material. Through modeling the discharge process, a better understanding of the PD phenomena and the mechanism may be attained to guide the maintenance and repair of the cable assets [2].

PD events in dielectric materials can be regarded as a process in which energy bursts out in the form of pulses. A discharge source can be considered as containing an electromagnetic wave source and an ultrasonic wave source. The characteristics of PD events are related to the applied voltage, load current, and ambient temperature of the cable insulation. In practical measurements, very good conditions or very poor conditions of cable insulation are easily determined by several indicators of PD events, while the assessment of intermediate states between the two extreme conditions is difficult [3]–[5]. Previously published PD methods can be divided into three categories:

a) Phase resolved analysis method [6]. This method relies on the phase relationship between PD signals and the test voltage signals that are quantified as the discharge magnitude q, the phase angle φ (or discharge time), and the discharge density n, acquired over selected time intervals. The prevalent PD measurement methods, phase-resolved partial discharge (PRPD) map and $\varphi - q - n$ map analysis, were based on this principle and mainly used in offline testing.

b) Time domain analysis method [7]. This type of method mainly displays the real discharge waveform with respect to the magnitude q and time t, which is more intuitive than the phase analysis method due to the correlation of the defect characteristics and the shape of the PD signal waveform.

The associate editor coordinating the review of this manuscript and approving it for publication was Pavlos I. Lazaridis.

c) Defect analysis method [8], [9]. This kind of method mainly focuses on the relationship between the PD charges and the test voltage. The abc-model [8], based on classical circuit theory, can only explain the PD process qualitatively. The apparent discharge amount in the model is much smaller than the amount of actual discharge. The dipole model is based on the electromagnetic field principle and obeys the gas discharge theory. The PD discharge magnitude in the dipole model [9] is equal to the amount of apparent discharge, and the quantitative relationship between the PD magnitude and the inception voltage can be deduced. However, interpretation of the results was reportedly limited by the defect location and cable size.

The above-described models only considered the relationship between PD events and discharge-inducing factors (various defects). They all ignored the process of discharge initiation and development. Consequently, the proposed PD methods may only indicate whether the condition of a cable insulation is good, operable or not, while the conditions between the two extreme conditions remain impossible to evaluate. In this paper, the characteristics of electric current associated with the PD process are summarized and analyzed, and a stage model of the PD current based on F distribution is proposed. The model can identify the three stages of PD development based on the current waveform, thereby helping to diagnose the degree of insulation defects.

II. PD MECHANISMS IN POWER CABLES

PD events can occur in gaseous, liquid, and solid insulating materials. According to the IEC 60270 standard [10], PD is a partial dielectric breakdown of the insulating material between two conductors. A prerequisite of the PD process in an insulation cavity is the initial free electrons. Usually generated near the cathode, the electrons help excite the electron avalanche while propagating to the anode and induce the discharge. When a PD event occurs in a cavity, which is regarded as a short gap, there are various forms of gap discharges. A discharge in a short gap is essentially Townsend discharge, if it requires free electrons emitted by the cathode to maintain the discharge [11]. Rapid discharge with the characteristics of fast rise time and large discharge magnitude was deemed as streamer discharge in several references. However, this view only considered the similarity of this kind of spark discharge and long gap streamer discharge, while their principles are different. Streamer discharge, in contrast to Townsend discharge, is associated with the photoionization process in the air gap and does not need the cathode to emit free electrons [12].

There is a minimum breakdown voltage $V_{paschen}$, which is known as the PD inception voltage (PDIV), in the process from the generation of initial free electrons to the occurrence of PD in an insulation defect. The PDIV is related to the type, composition, temperature, and pressure of the gas in the defect cavity. Reference [13] presented the Paschen curve of gaps of different sizes, and provided the breakdown field strength of the air gap required under certain pressure and size.

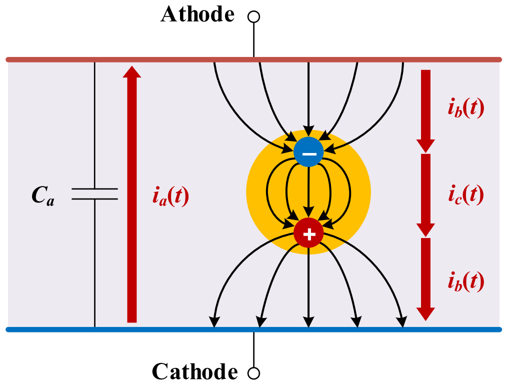

FIGURE 1. Schematic diagram of the PD mechanism in cable insulation.

The breakdown voltage of a certain volume of gas can be expressed by Paschen's law, as in (1):

$$V_{Paschen} = \frac{a \cdot p \cdot d}{b + \ln(p \cdot d)} \tag{1}$$

where d represents the diameter of the air gap, p represents the pressure of the gas, a and b are constants depending on the gas type.

PD is a rapid, transient process, which is the result of dipoles created by charge carriers of opposite polarity deposited on the internal surface of an insulating cavity [14], as in Figure 1. These charges generate an electrostatic Poisson field. The polarity of the electric field is opposite to the polarity of the Laplace field generated by the applied voltage. The ionization of the gas molecules in the cavity quenches suddenly, and the process may only last a few nanoseconds [15].

Taking the number of n_i neutral particles as an example, PD occurs when the number of ionized neutral gas particles exceeds a critical value. In the process, each neutral particle releases a single electron and a positive ion. The energy required for the displacement of the electron to the cavity wall by the electric field Coulomb force is given as in (2) [15], where E_i is the field strength corresponding to PDIV. According to the principle of potential energy doing work, W_i can also be expressed in (3). Therefore, the amount of PD charges can be obtained from the PDIV and the corresponding field strength, as in (4). Where m_d is the dipole moment generated by the dipole, e is the charge of the electron, and d_c is the diameter of the cavity.

$$W_i = n_i \cdot e \cdot E_i \cdot d_c \tag{2}$$

$$W_i = q_c \cdot V_i \tag{3}$$

$$q_c = n_i \cdot e \cdot d_c \cdot \frac{E_i}{V_i} = m_d \cdot \frac{E_i}{V_i} \tag{4}$$

When a PD event occurs in a cavity with a distance r_c from the center, as in Figure 2, the relationship between the PD inception field strength and the corresponding applied PDIV is given in (5). Where k_ε is the electric field enhancement

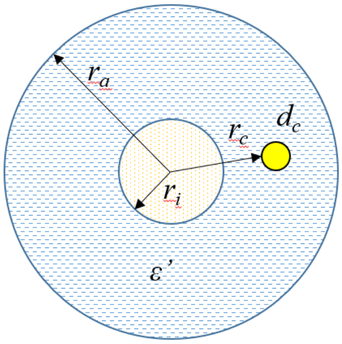

FIGURE 2. Schematic diagram of partial discharge in a hollow cavity of a coaxial insulator.

coefficient, which can be obtained from (6). For a piece of cross-linked polyethylene (XLPE) insulating material with a relative dielectric constant of 2.3, the value of k_ε is 1.23.

$$\frac{E_i}{V_i} = k_\varepsilon \cdot \frac{1}{r_c \cdot \ln(r_a/r_i)} \tag{5}$$

$$k_\varepsilon = \frac{3\varepsilon_r}{1+2\varepsilon_r} \tag{6}$$

III. PD DEVELOPMENT PROCESS IN POWER CABLES

A large number of research results on PD mechanism analysis, testing, modeling and simulation have been published, and PD measurements have also been used as condition indicators in many standards [3], [4], [9], [17]. The assessment of the criticality of PD defect site(s) are still inconclusive though. There have been no mathematical models representing the discharge process using gas discharge theory, and with the plasma theory the parameters of gas reaction that the model required cannot be easily obtained. By studying the vast amount of published PD research results, in this paper it is summarized that the PD development process in the insulation of power cables may be divided into three stages as in Figure 3.

Since a prerequisite of the PD process in an insulation cavity is the initial free electrons generated near the cathode. The initiation and progress to solid insulation breakdowns regarded as mainly including the following five main stages in this paper: A) directional movement of electrons; B) polymer oxidation or ion impact degradation; C) pitting corrosion; D) tree growth; and E) breakdown. The process of tree growth is not considered in this paper due to its short duration from growth to breakdown. Rather the paper will focus on whether the directional movement of electrons can be self-sustained. The first three of the five main stages (Stage A, B, and C) are the research objects of the paper. In Stage A, the PD activity will disappear immediately if the degree of insulation degradation is insignificant so that the directional movement of the electrons cannot self-sustained. Several international standards [3], [4], [9], [17] used parameters to define the standard waveform of PD pulses, as shown in Figure 4. PD activities in Stage A, characterized by a steep wave front and short duration, was also commonly regarded as a single

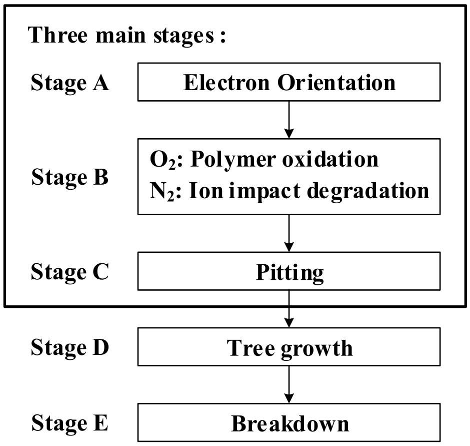

FIGURE 3. Schematic diagram of the cable partial discharge in stages with indication of the three main stages.

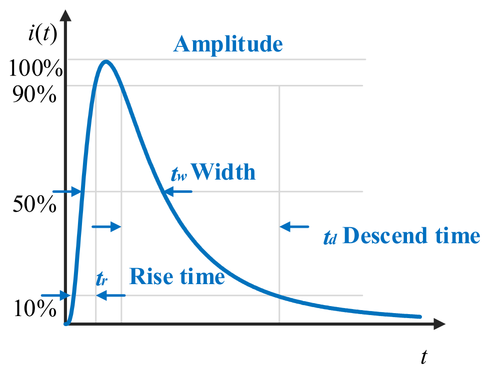

FIGURE 4. The typical waveform of the partial discharge in Stage A.

PD pulse. For a given discharge gap, the magnitude of a single discharge is approximately constant.

Highly oxidized products are produced during discharges: O, O_3, and O_2^-, if oxygen is involved in the reaction. Hydrogen, carbon monoxide, methane, and carbon dioxide are produced due to chemical reactions in the gas phase, and these products can react with polymer-free radicals to form acids. These acids are conductive, and it is speculated that they reduce the voltage across the void and help quench the discharge [20], [21]. The initially air-filled voids could be uniformly oxidized within a layer of several picometers thickness [22]. The bombardment of nitrogen ions will further aggravate the deterioration of the insulation when all the oxygen is consumed, then the discharge enters into Stage B. A typical waveform of this stage is shown in Figure 5.

The discharge process in Stage B is longer than Stage A, and the formation of the discharge is a slow process. The rise time of pulses in Stage B can be hundreds of times of that in Stage A. Contrary to the streamer-like pulse discharge in Stage A, the magnitude distribution of Townsend-like discharges in Stage B is wider. The discharge process in Stage B may be accompanied by the formation of oxalic acid crystals [9], [23], which tend to grow with continued discharge activity which then leads to Stage C.

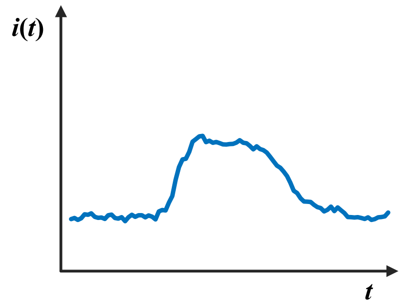

FIGURE 5. The typical waveform of the partial discharge in Stage B.

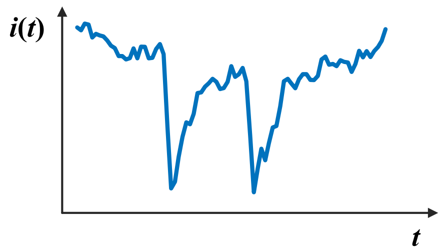

FIGURE 6. The typical waveform of the partial discharge in Stage C.

PD activities in Stage C may be characterized by a small pulse height, high repetition rate, and up to several discharges per microsecond [24]. The rise time of the discharge in Stage C is comparable to that of in Stage A, but the decay time is much longer, as in Figure 6. Discharges in Stage C lead to localized micro ablation of the dielectric.

IV. A F DISTRIBUTION BASED MODEL FOR CLASSIFICATION OF 3 STAGES OF PD ACTIVITIES

In order to unify the current characteristics of the above three stages in one model, the F distribution is proposed to fit their waveforms. The F distribution is the sampling distribution of the ratio of two independent random variables that obey the chi-square distribution divided by their degrees of freedom. Let $X = \chi^2(n_1)$, $Y = \chi^2(n_2)$, X and Y are independent of each other. Then $F = (X/n_1)/\ (Y/n_1)$ is said to obey the degrees of freedom n_1 and n_2 of the F distribution, denoted as $F(n_1, n_2)$. The probability density function of the F distribution is provided in (7). The PD waveform of Stage A has many similarities with the F distribution. First of all, the PD current in Stage A can be written in the mathematical form of F distribution, for example, the discharge current waveform $i(t)$ obeys the F distribution with degrees of freedom of 12 and 6, i.e. $i(t) = F$ (12,6). In terms of the physical mechanism, the PD current in Stage A has the equation of the electron motion formed from the first electron directional motion, and can be regarded as a combination of multiple normal random variables (electrons) as well. Stage B and Stage C can be regarded as the superposition of multiple Stage A, the specific waveform depends on the way and amount of superposition. The development of a PD process means the increase the number of discharges and change in the discharge waveforms, which also correspond to the increase of the freedom degree in the F distribution. Specifically, the comparison of a PD in Stage A and the F distribution is demonstrated in Table 1, the comparison of PD in each of the three stages is given in Table 2.

TABLE 1. Comparison of the PD in Stage A and F distribution.

The PD in Stage A	F distribution
Electronic	Random variable X
Current	Probability density function (PDF)
Discharge magnitude	Cumulative distribution function (CDF)
Four parameters: t_r, t_d, t_w, I_m	Two parameters n_1, n_2

$$f(x, n_1, n_2) = \begin{cases} \dfrac{\Gamma\left(\frac{n_1+n_2}{2}\right)\left(\frac{n_1}{n_2}\right)^{\frac{n_1}{2}} x^{\frac{n_1}{2}-1}}{\Gamma\left(\frac{n_1}{2}\right)\Gamma\left(\frac{n_2}{2}\right)\left(1+\frac{n_1 x}{n_2}\right)^{\frac{n_1+n_2}{2}}} & , x > 0 \\ 0 & , x \le 0 \end{cases} \quad (7)$$

For PD activities in Stage A, as in Table 1, the integral of the current over time is the discharge magnitude, which is a fixed value P_c with assumption of no change in size of defect site(s). For the F distribution, the integral of the probability density function over the chosen variable is the distribution function, and the whole integral value is 1. For the PD in Stage A, the current is assumed to be due to electron movement, the charge of a single electron is constant, and the integral of the current over time is the discharge magnitude.

The waveform of the PD in each of the three stages has its unique characteristics, as presented in Table 2. The main feature of the waveform in Stage A is that it appears in the form of a single pulse, and one F distribution function can fit the waveform. The waveform in Stage B presents the form of multiple discharge superposition, which is formed by the N ($N \gg 1$) number superposition of F distribution functions. The waveform in Stage C is in the form of several ($N \geq 1$) single pulses reversed along the y axis.

V. CASE STUDY AND MODEL COMPARISON

A. CASE STUDY

The structure and size parameters of a medium-voltage single-core XLPE cable selected in the case study of this article are listed in Table 3 and Figure 7, respectively. The defect location and size parameters involved in the calculation are listed in Table 4.

From the Paschen curve of air, a can be taken as 365 ($V\cdot cm^{-1}\cdot Torr^{-1}$) and b as 1.18 ($cm^{-1}\cdot Torr^{-1}$) in a dry environment at room temperature. The result is shown in Figure 8. At 0.836 Torr·cm, the minimum breakdown voltage across the gap, assuming air as the content in the gap, is 305.3 V.

TABLE 2. Comparison of PD in the three stages.

Three stages of PD	Features of the waveform	The superposition number N of F distribution
Stage A	Single pulse	$N = 1$
Stage B	Multiple discharge	$N >> 1$
Stage C	Reverse pulse	$N \geq 1$

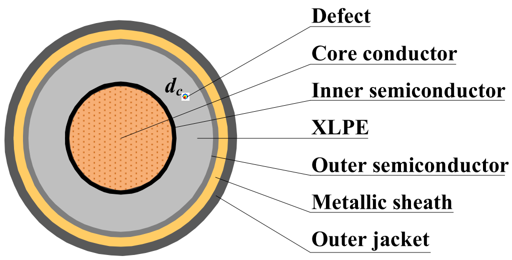

FIGURE 7. Construction of single-core XLPE cable.

TABLE 3. Parameters of XLPE cable.

Core material	Copper (Cu)
Insulation material	XLPE
Protective layer material	Copper (Cu)
External insulation material	Polyvinyl chloride (PVC)
Cable core wire cross-sectional area	500 mm^2
Insulation thickness	8 mm
Protective layer thickness	0.1 mm
Total diameter	40 mm

In the case of considering the development of discharge process, the discharge current is the derivative of the discharge magnitude and is also a function of time. In this paper, electrons are mainly assumed as carriers, and the distribution of electrons in insulation defects is used to simulate each discharge stage (Stage A, Stage B, and Stage C), and the corresponding current waveforms are calculated based on the above models. As shown in Figure 7, the two-dimensional cross-section of the defect is a circle with a diameter of 0.1 mm, and the center of the defect circle is 14.32 mm away from the core conductor. The defect is directly subjected to a direct current stress, and the corresponding cathode becomes the course of electron emission, which corresponds to the lower half of the defect in the simulation.

In the simulation with the determined structure and given voltage level of the cable, the electrical stress in the defect is relatively fixed, and the time of the partial discharge process is very short relative to the duration it takes for the macroscopic electrical stress to change. Therefore, the change of the macroscopic electrical stress can be ignored. According to the gas discharge theory, the discharge process of the tiny air gap mainly corresponds to the directional movement of carriers. In the case the typical current waveform in the discharge stage is basically determined, the electron distributions of the defect in each stage can be simulated by using the current

TABLE 4. Parameters of XLPE cable defect and material.

Insulation outer radius	r_a = 20.62 mm
The inner radius of the insulation	r_i = 12.62 mm
Defect location	r_c =14.32 mm
Defect diameter	d_c = 0.1 mm
XLPE relative permittivity	$\varepsilon_r = 2.3$
The critical value of the ionization number of gas molecules	$n_i = 10^8$
Reference temperature	20 °C
Loading	100 %

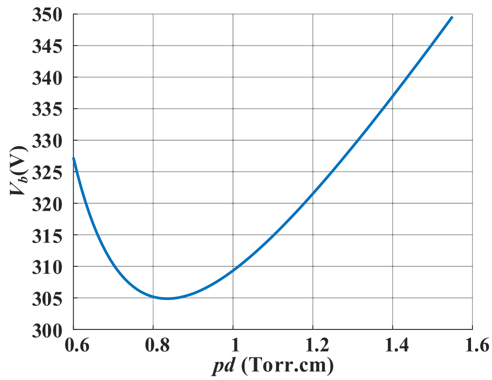

FIGURE 8. Paschen curve in dry air at room temperature.

waveform in the model. In this example, for the PDs in stage A, it is assumed that only one pulse is induced each time. Compared with the power frequency cycle, the duration of a single partial discharge is very short compared with the duration between PD pulses, so it can be assumed that the electrical stress on the defect does not change with time during the discharge. The discharge current in Stage A obeys the F distribution with 12 and 6 degrees of freedom, the electron distribution corresponding to the formation of stable discharge is shown in Fig. 9(a), and the discharge current $i(t)$ is $F(12,6)$, as in Figure 9(b), where the x axis corresponds to the time, in ns, and the y axis corresponds to the current i, in mA.

The main process of discharges in Stage B is only polymer oxidation/ion shock degradation. In this example, stage B was composed of 64 discharge pulses superimposed. The electron distribution in the defect is shown in Fig. 10(a), and the discharge current is shown in Fig. 10(b). Due to the large number of discharges set by the simulation, relatively the peak of the waveform or the flat area in the middle of the waveform is longer.

Stage C is the stage where the discharge is more unstable, the physical process is pitting, tree growth is about to occur. The discharge waveform in Stage C also has its unique characteristics. Its reverse waveform in y-axis is similar to the current pulse of PDs in Stage A. The electron distribution in this stage is shown in Fig. 11(a), and the discharge current is shown in Fig. 11(b).

In waveform identification, the discharge stages can be distinguished first. If the waveform is in the form of a single

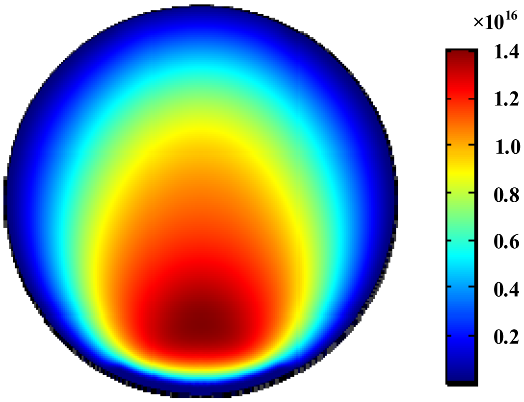

(a)

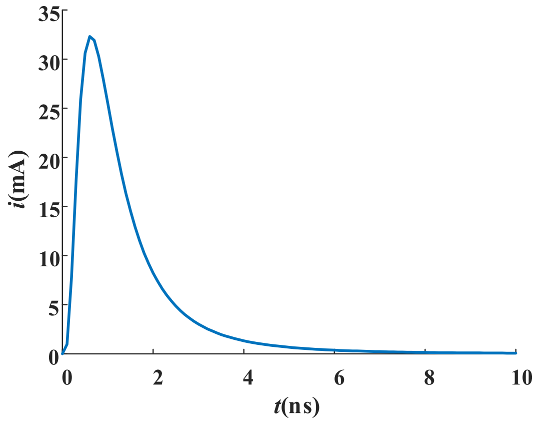

(b)

FIGURE 9. (a) The electron distribution at Stage A. (b) The simulation curve of PD current at Stage A.

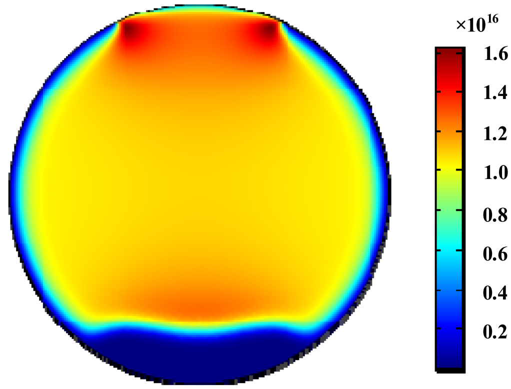

(a)

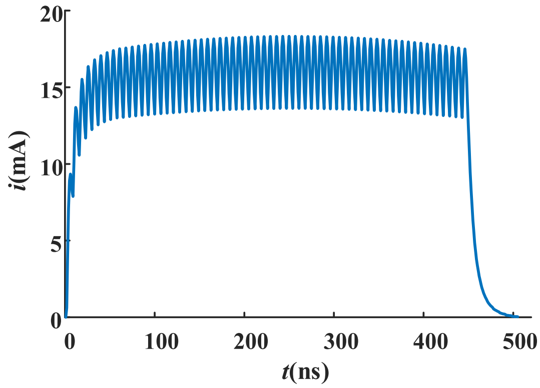

(b)

FIGURE 10. (a) The electron distribution at Stage B. (b) The simulation curve of PD current at Stage B.

pulse, use the F distribution function to fit the current waveform to obtain the fitting function $F_1(n_1, n_2)$ and confidence of the waveform. If the confidence level is high, the obtained current is considered to be the partial discharge current in Stage A. If the waveform envelope of the waveform in the analysis interval is always at a position greater than 0, and the fitting function conforms to the superposition feature of multiple F distributions, the obtained current is considered to be the partial discharge current in Stage B. If the reverse of the y-axis of the waveform has the form of a single pulse, use the F distribution function to fit the current waveform (the reverse of the y-axis) to obtain the fitting function $F_3(n_3, n_4)$ and confidence of the waveform. If the confidence level is high, the obtained current wave is considered to be the partial discharge current in Stage C.

B. MODEL VALIDATION

As mentioned in section III, the typical waveforms of the partial discharges in the three stages were presented in Fig. 4∼6, which have been directly or indirectly validated in previous studies [3], [4], [9], [17], [20]–[24]. Therefore, the validation of the model is realized by comparing the waveform similarity of the three stages. Firstly, the key characteristics of the waveforms of each stage needs to be compared. The waveform of Stage A is mainly a single pulse, the waveform of Stage B is longer than the first stage and has an obvious plateau in the middle, and the waveform of Stage C contains several inverse pulses in series. It can be seen that the simulation results are consistent with previous studies in terms of key features.

In order to determine the similarity between the waveforms more specifically from the perspective of geometric features, the cosine similarity [25] is adopted here. The cosine similarity measures the similarity between two vectors by calculating the cosine value of the angle between the two vector inner product spaces, and its expression is shown in (8).

$$\cos(\theta) = \frac{\sum_{i=1}^{n} (x_i, y_i)}{\sqrt{\sum_{i=1}^{n} x_i^2}\sqrt{\sum_{i=1}^{n} y_i^2}} \tag{8}$$

Among them, n is the number of sampling points of variables $\boldsymbol{x} = [x_1, x_2, \ldots, x_n], \boldsymbol{y} = [y_1, y_2, \ldots, y_n]$ under consideration. When $\cos(\theta) = -1$, it means that directions of the overall change in $\boldsymbol{x}$ and $\boldsymbol{y}$ are completely opposite, and the similarity is the most negative. When $\cos(\theta) = 1$, it means that the directions of overall change in the two variables is exactly the same, and the similarity is the strongest. When the absolute

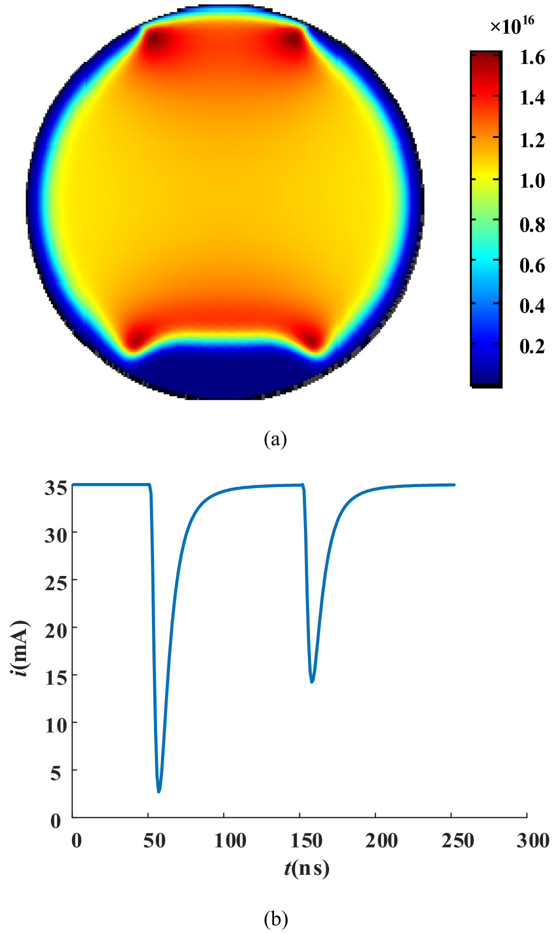

FIGURE 11. (a) The electron distribution at Stage C. (b) The simulation curve of PD current at Stage C.

value of $\cos(\theta)$ is close to 0, it means that the difference between the two variables is large, and the similarity is weak.

In the case study, the cosine similarities of the three stage waveforms are 0.9969, 0.8025, 0.9228, respectively. They are all greater than 0.8, which means the overall similarity of the waveforms calculated by the model is relatively high, and the results are relatively credible. Then the waveforms of each stage for the F distribution of 5 groups of different parameters have been simulated, and the similarity results can be shown in Table 5.

It can be seen that in the comparison of the F distribution waveform similarity of the five group parameters, ($n_1 = 12$, $n_2 = 6$) has the highest overall similarity.

C. MODEL COMPARISON

At present, partial discharge models based on defect analysis are mainly divided into models based on equivalent circuits and models based on electric dipoles. Here, the abc model and the electric dipole model are selected as the typical models, which are compared and analyzed with the model proposed in this paper.

In the abc model, the cable with defects is equivalent to a series-parallel structure of a capacitance, and the change of

TABLE 5. The similarity results for the f distribution of 5 groups of different parameters.

$F(n_1, n_2)$	Stage A	Stage B	Stage C
n_1=8, n_2=4	0.9950	0.7833	0.9194
n_1=5, n_2=5	0.9768	0.7816	0.9136
n_1=10, n_2=5	0.9969	0.7828	0.9203
n_1=12, n_2=6	0.9969	0.8025	0.9228
n_1=15, n_2=10	0.9744	0.7902	0.9134

the equivalent capacitance parameters is used to simulate the degree of defects. As shown in Fig. 12(a), the capacitance of the part without defects in the cable insulation is represented by C_a' and C_a'', the part containing void defects is represented by capacitance C_c, and the parts at both side of the void are represented by capacitance C_b' and C_b'' respectively. In the equivalent circuit, as shown in Fig. 12(b), the total capacitance with C_a' and C_a'' being added in parallel is represented by C_a, and the total capacitance including C_b' and C_b'' is represented by C_b. The voltage applied across the insulation is represented by V_a. When the air gap in the insulation breaks down, the voltage across the capacitor C_c changes by ΔV_c, and the internal discharge is given in (9).

$$q_c = \Delta V_C \left(C_c + \frac{C_a \cdot C_b}{C_a + C_b} \right) \tag{9}$$

$$q_a = \Delta V_a \cdot C_a = \frac{C_a \cdot C_b}{C_a + C_b} \cdot \Delta V_c \tag{10}$$

In (9), the PD charges of the abc model mainly depends on the unpredictable factors C_b and C_c. Therefore, (10) is often used instead of (9) in practical applications. However, the discharge loop and the series loop of the equivalent capacitor are not in the same loop. According to the voltage division relationship in the circuit, the value of q_c will be larger than q_a.

In the electric dipole model, the PD charges can be presented in (4), and basic idea was expressed in section II. The calculation results in the case study and the specific characteristics can be shown in Table 6.

The abc-model is based on classical circuit theory, but can only explain the PD process qualitatively. And the apparent discharge magnitude is smaller than the actual discharge amount in the model. The dipole model is based on the electromagnetic field principle and obeys the gas discharge theory. The PD magnitude in this model is equal to the apparent discharge magnitude, and the quantitative relationship between the PD magnitude and the discharge starting voltage can be deduced, but the explanation of results may be impossible without knowing the defect location and cable size. However, these two models are directly derived from theory and can hardly be verified in engineering practice; and the models themselves rely too much on the location of defects and cable size, and do not consider the development of partial discharge process. The model proposed in this

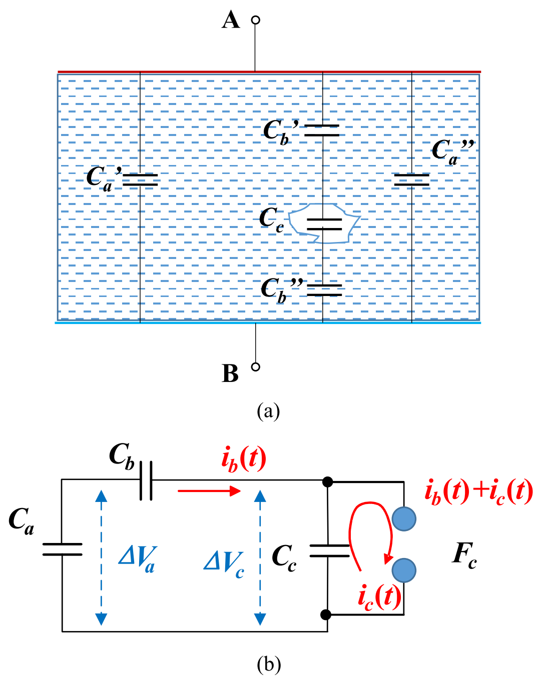

FIGURE 12. (a) Schematic diagram of the of the abc model. (b) The equivalent circuit of the abc model.

TABLE 6. Comparison among three PD models.

Considerations in Models	abc	dipole	This paper
Discharge magnitude (pC)	40.71	46.65	46.65
Apparent discharge	×	√	√
Different stages of PD	×	×	√
Electron distribution	×	×	√

paper can display the electron distribution form and discharge current waveform in typical defects of three stages of partial discharge development, and is functionally superior to the previous two models, in terms of practical applications.

VI. CONCLUSION

In this paper, the mechanism of PD development process in power cables is summarized and analyzed. A revised model based on F distribution is proposed with consideration of the three different stages in the PD development process, which is able to reveal the criticality of the cable insulation deterioration. Specifically, there are the following conclusions:

1) The model proposed in this paper can effectively simulate the three stages of PD development, which is related to the degree of insulation deterioration.
2) The waveforms of each stage for the F distribution of 5 groups of different parameters have been simulated, the results indicate that F-distribution with degrees of freedom $n_1 = 12, n_2 = 6$ for the PD simulation is with the best similarity.
3) The model proposed in this paper can display the electron distribution and the PD current waveform in typical defects of three stages of the PD development, and is functionally superior to the abc model and the dipole model.

REFERENCES

[1] C. Zhou, H. Yi, and X. Dong, "Review of recent research towards power cable life cycle management," *High Volt.*, vol. 2, no. 3, pp. 179–187, Sep. 2017.
[2] A. Pedersen, I. W. McAllister, and G. C. Crichton, "Partial discharge detection: Theoretical and practical aspects," *IEE Proc.-Sci., Meas. Technol.*, vol. 142, no. 1, pp. 29–36, Jan. 1995.
[3] *IEEE Recommended Practice for Protection and Coordination of Industrial and Commercial Power Systems (IEEE Buff Book)*, IEEE Standard 242-2001 (Revision of IEEE Standard 242-1986), Dec. 17, 2001, pp. 1–710.
[4] *IEEE Standard for High-Voltage Switchgear (Above 1000 V) Test Techniques–Partial Discharge Measurements*, IEEE Standard C37.301, Mar. 20, 2009, pp. 1–72.
[5] P. Morshuis, "Partial discharge mechanisms," Delft Univ. Technol. (TuDelft), Delft, The Netherlands, Tech. Rep., 1993.
[6] X. Peng, C. Zhou, D. M. Hepburn, M. D. Judd, and W. H. Siew, "Application of K-means method to pattern recognition in on-line cable partial discharge monitoring," *IEEE Trans. Dielectr. Electr. Insul.*, vol. 20, no. 3, pp. 754–761, Jun. 2013.
[7] B. Sheng, C. Zhou, D. M. Hepburn, X. Dong, G. Peers, W. Zhou, and Z. Tang, "Partial discharge pulse propagation in power cable and partial discharge monitoring system," *IEEE Trans. Dielectr. Electr. Insul.*, vol. 21, no. 3, pp. 948–956, Jun. 2014.
[8] L. Niemeyer, "A generalized approach to partial discharge modeling," *IEEE Trans. Dielectr. Electr. Insul.*, vol. 2, no. 4, pp. 510–528, Aug. 1995.
[9] S. Chen and T. Czaszejko, "Partial discharge test circuit as a spark-gap transmitter," *IEEE Elect. Insul. Mag.*, vol. 27, no. 3, pp. 36–44, May 2011.
[10] *Partial Discharge Measurements, Third Edition. London: International Electrotechnical Commission (IEC)*, IEC Standard 60270, 2000.
[11] R. Bartnikas, "Partial discharges. Their mechanism, detection and measurement," *IEEE Trans. Dielectr. Electr. Insul.*, vol. 9, no. 5, pp. 763–808, Oct. 2002.
[12] P. Morshuis, "Partial discharge mechanisms in voids related to dielectric degradation," *IEE Proc. Sci. Meas. Technol.*, vol. 142, no. 1, pp. 62–68, Jan. 1995.
[13] A. Pedersen, G. C. Crichton, and I. W. McAllister, "Partial discharge detection: Theoretical and practical aspects," *IEE Proc. Sci., Meas. Technol.*, vol. 142, no. 1, pp. 29–36, 1995.
[14] E. Lemke, "A critical review of partial-discharge models," *IEEE Elect. Insul. Mag.*, vol. 28, no. 6, pp. 11–16, Nov. 2012.
[15] E. Lemke, "Analysis of the partial discharge charge transfer in extruded power cables," *IEEE Elect. Insul. Mag.*, vol. 29, no. 1, pp. 24–28, Jan. 2013.
[16] G. A. Dawson and W. P. Winn, "A model for streamer propagation," *J. Phys.*, vol. 183, no. 2, pp. 159–171, 1965.
[17] *Electric Cables—Calculation of the Current Rating—Part1-1: Current Rating Equations (100% Load Factor) and Calculation of Losses—General*, document IEC 60287-1-1:2006+A1:2014, 2014.
[18] X. Xu and D. Zhu, *Gas Discharge Physics*. Shanghai, China: Fudan Univ. Press, 1996.
[19] J. Chen, *Low Temperature Plasma Chemistry and its Application*. Beijing, China: Science Press, 2001.
[20] M. Gamez-Garcia, R. Bartnikas, and M. Wertheimer, "Synthesis reactions involving XLPE subjected to aartial discharges," *IEEE Trans. Electr. Insul.*, vol. EI-22, no. 2, pp. 199–205, Apr. 1987.
[21] X. Zhou, C. Zhou, and I. J. Kemp, "An improved methodology for application of wavelet transform to partial discharge measurement denoising," *IEEE Trans. Dielectr. Electr. Insul.*, vol. 12, no. 3, pp. 586–594, Jun. 2005.
[22] S. Biswas, D. Dey, B. Chatterjee, and S. Chakravorti, "An approach based on rough set theory for identification of single and multiple partial discharge source," *Int. J. Electr. Power Energy Syst.*, vol. 46, pp. 163–174, Mar. 2013.
[23] W. McDermid and J. C. Bromley, "Partial discharge screening test for internal voids and delaminations in stator coils and bars," *IEEE Trans. Energy Convers.*, vol. 14, no. 3, pp. 292–297, Sep. 1999.

[24] S. B. Lee, A. Naeini, S. Jayaram, G. C. Stone, and M. Sasic, "Surge test-based identification of stator insulation component with partial discharge activity for low voltage AC motors," *IEEE Trans. Ind. Appl.*, vol. 56, no. 3, pp. 2541–2549, May 2020.
[25] S. K. Biswas and P. Milanfar, "One shot detection with Laplacian object and fast matrix cosine similarity," *IEEE Trans. Pattern Anal. Mach. Intell.*, vol. 38, no. 3, pp. 546–562, Mar. 2016.

GEN LI was born in China. He received the B.Sc. degree from the Huazhong University of Science and Technology, Wuhan, China, in 2017, and the master's degree from the Wuhan Research Institute of Posts and Telecommunications, Wuhan, in 2021. He is currently pursuing the Ph.D. degree with Wuhan University, Wuhan. His research interests include fault location and condition monitoring of power cables.

JIE CHEN, photograph and biography not available at the time of publication.

HONGZE LI, photograph and biography not available at the time of publication.

LIBIN HU, photograph and biography not available at the time of publication.

WENJUN ZHOU (Senior Member, IEEE) was born in China, in July 1959. He received the Ph.D. degree in hydraulic and electrical engineering from the Wuhan University of Hydraulic and Electrical Engineering, Wuhan, China, in 1990. He is currently a Professor with the School of Electrical Engineering and Automation, Wuhan University. He is also the Vice Director of the Hubei High Voltage Committee. His research interests include lightning protection and the diagnostic techniques for outdoor electrical insulations. He is a member of the High Voltage Committee, Chinese Society of Electrical Engineering (CSEE), the Electrotechnical Test and Measurement Committee, China Electro-technical Society (CES), and the China Lightning Protection Standard Committee.

CHENGKE ZHOU received the B.Sc. and M.Sc. degrees in electrical engineering from the Huazhong University of Science and Technology, China, in 1983 and 1986, respectively, and the Ph.D. degree from The University of Manchester, U.K., in 1994. Since 1994, he was a Lecturer with Glasgow Caledonian University (GCU). He was a Senior Lecturer with Heriot-Watt University. In 2007, he returned to GCU, as a Professor. He is currently a Professor with the School of Electrical Engineering, Wuhan University. He has published more than 180 articles in the area of PD-based condition monitoring of MV/HV plant and power system analysis. He is a fellow of the IET.